Journal of Hydrology 544 (2017) 306–318

Contents lists available at ScienceDirect

Journal of Hydrology

journal homepage: www.elsevier.com/locate/jhydrol

Research papers

Anthropogenic warming has caused hot droughts more frequently in China

Huopo Chen *, Jianqi Sun

Nansen-Zhu International Research Centre, Institute of Atmospheric Physics, Chinese Academy of Sciences, Beijing, China
Joint Laboratory for Climate and Environmental Change at Chengdu University of Information Technology, Chengdu, China
Collaborative Innovation Center on Forecast and Evaluation of Meteorological Disasters, Nanjing University of Information Science & Technology, Nanjing, China

ARTICLE INFO

Article history:
Received 7 September 2016
Received in revised form 20 November 2016
Accepted 21 November 2016
Available online 23 November 2016
This manuscript was handled by A. Bardossy, Editor-in-Chief

Keywords:
Hot drought events
Natural variability
Anthropogenic warming
Risk
China

ABSTRACT

Historical records have indicated an increase in high-impact drought occurrences across China during recent decades, but whether this increase is due to natural variability or anthropogenic change remains unclear. Thus, the shift toward dry conditions and their associated attributions across China are discussed in this study, primarily regarding the standardized precipitation evapotranspiration index (SPEI). The results show that drought occurrences across China increased consistently during 1951–2014, especially during the recent twenty years. Most of the increased drought events happened under warm-dry conditions that coincided with relatively high temperature anomalies but without large anomalies in annual precipitation, implying an increase in hot drought events across China. Further analysis revealed that the change in drought occurrences were mainly due to the combined activity of external natural forcings and anthropogenic changes across China. However, external natural forcings were mainly responsible for the variability of droughts and anthropogenic influences for their increasing trends, suggesting that anthropogenic warming has increased hot drought occurrences, associated risks and impacts across China. With continued warming in the future, the impact of anthropogenic warming on the increased hot drought events will be further amplified. The probability of warm years is projected to significantly increase, and the occurrence probability of hot drought events (SPEI < −1.0) will increase to nearly 100% by the year 2050, even though the annual precipitation is projected to increase across China in the future.

1. Introduction

In recent decades, China has suffered several prolonged extreme droughts, such as the ones from the autumn of 2009 to the spring of 2010 in Southwest China, from July to August of 2013 in Eastern China, and from July to August of 2014 in North China, which have resulted in large economic losses, ecosystem damage, and the disruption of society (e.g., Yang et al., 2012; Sun, 2014; Wang and He, 2015; Wang et al., 2015). According to Chinese governmental statistics, the severe drought in 2009/2010 in Southwest China caused a shortage of drinking water that impacted more than 21 million people and 11 million livestock, resulting in economic losses that reached nearly 30 billion US dollars (e.g., Yang et al., 2012). Additionally, the drought in North China in the summer of 2014 is considered to be the most serious event in the past six decades, resulting in a devastating reduction of agricultural production (Wang and He, 2015). Furthermore, the study by Yu et al. (2014) has revealed that severe and extreme droughts have become more serious since the late 1990s in China, and the dry areas were reported to increase by ~3.72% decade^{-1} in past decades. Thus, understanding the causes of the increasing severe drought events in China is urgently important for improving predictions and reducing economic losses.

Previous studies have revealed the possible physical mechanisms responsible for severe drought in China, through associated atmospheric circulation patterns and atmosphere/ocean modes (e.g., Wang, 2001; Ma, 2007; Gao and Yang, 2009; Yang et al., 2012; Wang and He, 2015). The weakening of the East Asian monsoon after the late 1970s has contributed to a dramatic decrease of monsoon rainfall in North China, resulting in the so-called "Southern Flood—Northern Drought" pattern over eastern China (Wang, 2001, 2002; Ding et al., 2009). The winter North Atlantic Oscillation (NAO) also showed an in-phase correlation with summer precipitation in eastern China, with the NAO directing precipitation for 2–3 years (Fu and Zeng, 2005). Furthermore, from a multi-decade

* Corresponding author at: Nansen-Zhu International Research Centre (NZC), Institute of Atmospheric Physics, Chinese Academy of Sciences, PO Box 9804, Beijing 100029, China.
E-mail address: chenhuopo@mail.iap.ac.cn (H. Chen).

http://dx.doi.org/10.1016/j.jhydrol.2016.11.044
0022-1694/

perspective, the positive phase of the Pacific Decadal Oscillation (PDO) generally corresponds to a dry period over North China (Ma, 2007; Pei et al., 2015). The severe drought over Southwest China during the 2009/2010 autumn-winter was simultaneously accompanied by a strong negative-phase Arctic Oscillation and an El Niño Modoki event (Yang et al., 2012). The snow cover anomaly over the Tibetan Plateau and the activity of the Western Pacific Subtropical High are also considered as two important causes of the droughts in this region, especially the drought in the summer of 2006 (Zou and Gao, 2007). Additionally, some studies have emphasized the impacts of the upper tropospheric jet stream on precipitation anomalies over central-southern China (e.g., Wang et al., 2010).

Despite good insights into the causes of droughts based on large-scale atmospheric circulation anomalies, the influence of anthropogenic forcings on the occurrence probability of droughts has received less attention until recently (Li et al., 2015a; Zhao and Dai, 2015; Zhao et al., 2015). In early 2007, using a regional climate model study, Gao et al. (2007) showed that the precipitation decreased and the temperature increased when land use was modified by anthropogenic activities. Recently, Wang et al. (2013) implicated anthropogenic emissions as a prime driver of the "Southern Flood—Northern Drought" pattern in eastern China after the late 1970s. However, some recent analyses (Zhou et al., 2013; Song et al., 2014; Zhang and Zhou, 2015) from simulations of the Coupled Model Intercomparison Project phase 5 (CMIP5) argued that although the presence of aerosols can drive a weakened monsoon circulation, the responses from these models are far weaker than the observations. Moreover, the models failed to reproduce the observed precipitation changes as well as the drought trend in northern China. Therefore, they suggested that natural variability was the dominant factor that determined the drought changes in China and that the aerosol influence played only a complementary role. This discrepancy again raised the question of which factor is important for inducing the increasing droughts in China.

Precipitation deficits are a prerequisite for drought occurrences by any definition, and thus most previous efforts have evaluated the droughts using only precipitation anomalies (e.g., Yang et al., 2012; Chen et al., 2013; Zhang et al., 2013a; Li et al., 2015b). In addition, temperature anomalies are also considered to play an important role in drought occurrences, greatly amplifying evaporative demand and thereby increasing the overall drought intensity and impact (e.g., Dai et al., 2004; Dai, 2012; AghaKouchak et al., 2014; Chen and Sun, 2015a). In the past century, human activity has caused significant temperature increases. However, little attention has been given to the analysis of anthropogenic influences on droughts in China.

Therefore, on the basis of previous studies, this work focuses mainly on the discussion of changes in drought occurrences in China under warming conditions. More importantly, the possible impacts on the droughts from external natural and anthropogenic influences are separated and discussed. In addition, the probability of drought occurrence is also projected under continued future warming scenarios.

2. Data and methods

2.1. Datasets

The complete record sets, including monthly precipitation and temperature for the period from January 1951 to December 2014 from 160 first-order meteorological stations across China (Fig. 1), were used in this study. These stations are maintained by professional weather observers in China, and the data are collected and released by the National Climate Center along with their homogeneity and quality control processes. Because the climates in China vary across regions due to its complex topography, China is separated into six regions (Fig. 1) according to the China meteorological and geographical division handbook that was released by the National Meteorological Center of the China Meteorological Administration in 2006, which has been widely used in early studies (e.g., Chen et al., 2012a). These regions include Northeast China (NEC), North China (NC), South China (SC), Southwest China (SWC), eastern Northwest China (ENWC), and western Northwest China (WNWC). Analyses mainly focused on these six regions and are presented in the following sections. The time series were calculated from the averages of all stations for China as a whole and for each of six regions.

To assess the potential effects of natural and anthropogenic forcings on droughts, monthly outputs from 15 climate model simulations that include both external natural and human forcings ("Historical" experiment), only external natural forcings ("Natural" experiment; simply referring as NAT hereafter), and only anthropogenic influences ("GHG" experiment: Greenhouse Gases) were used in this study. Additionally, the 21st-century scenarios for future greenhouse gas emissions, RCP4.5 (Representative Concentration Pathways) and RCP8.5 as defined in Moss et al. (2010), were used in this study; 33 models from RCP4.5 and 28 models from RCP8.5 were selected to evaluate potential future changes of droughts in China. All these analyses in this study were based on the first ensemble member of each model, referred to as *r1i1p1* for all experiments. These outputs were extracted from the CMIP5 and are archived at the website of the Earth System Grid (ESG) gateway, hosted by the PCMDI (Program for Climate Model Diagnosis and Intercomparison). More information about these models is presented in Table 1. These monthly outputs were re-gridded into a common $2.5^\circ \times 2.5^\circ$ grid using a first-order conservative remapping procedure. The topographical adjustment was implemented for the re-gridded monthly temperature due to the different resolutions between models and the target grids.

2.2. Methods

Objectively quantification of drought occurrence, intensity, duration, and spatial extent is very complex. Thus, numerous studies have been devoted to improving drought detection and monitoring, and a few objective indices have been developed on the basis of readily available data (e.g. Palmer, 1965; McKee et al., 1993; Ma and Fu, 2001). Among these indices, the Palmer drought severity index (PDSI; Palmer, 1965) and the standardized precipitation index (SPI; McKee et al., 1993) are the two most widely used. However, more recent studies (e.g. Guttman, 1998; Dubrovsky et al., 2009; Vicente-Serrano et al., 2010; Beguería et al., 2014) have identified several deficiencies in these indices that limit their accuracies in both operational and research works. For example, the main shortcoming of the PDSI is its built-in fixed time scale of 9–12 months (Guttman, 1998), while for the SPI only precipitation variability is considered in its calculation, but the role of temperature is ignored (Vicente-Serrano et al., 2010). Therefore, a new standardized precipitation evapotranspiration index (SPEI) based on a simple water balance (i.e., the difference between precipitation P and potential evapotranspiration E) was developed by Vicente-Serrano et al. (2010) and further improved by Beguería et al. (2014).

The process of SPEI calculation can be summarized as follows. First, Vicente-Serrano et al. (2010) suggested the difference (Δ) of P and E to measure the water surplus or deficit:

$$\Delta_i = P_i - E_i \quad (1)$$

Second, Δ is aggregated at different time scale (n) as:

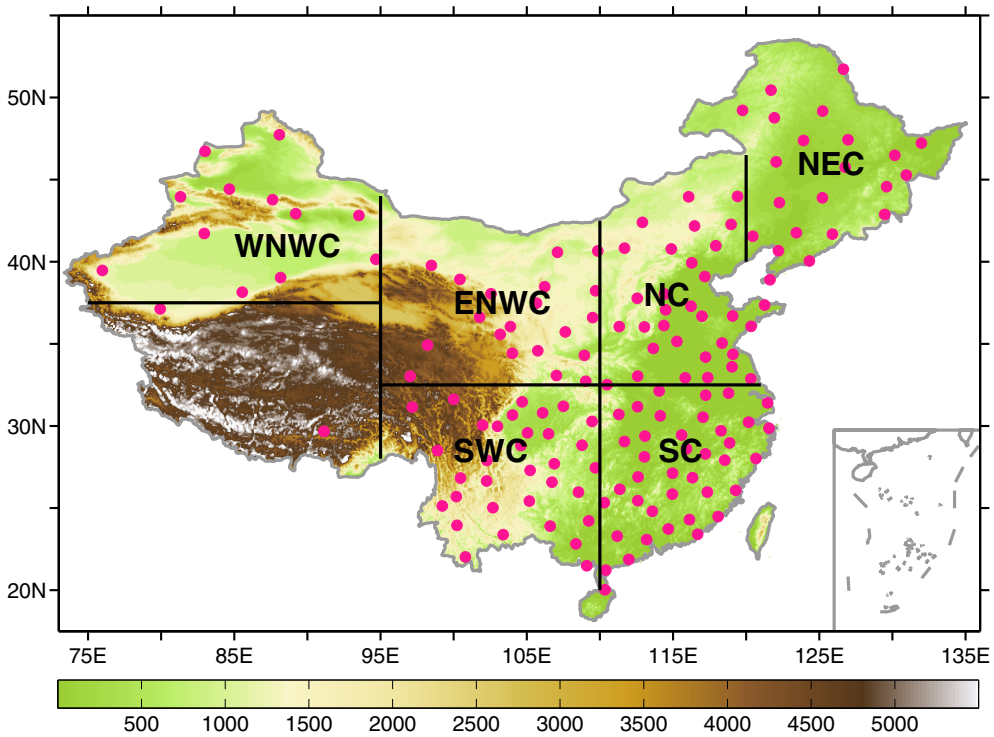

Fig. 1. Maps of locations of 160 meteorological stations and topography in China. Mainland China is divided into six regions, including Northeast China (NEC), North China (NC), South China (SC), Southwest China (SWC), eastern Northwest China (ENWC), and western Northwest China (WNWC). Units (topography): m.

Table 1
List of CMIP5 models used in this study. The label "√" means the model has been employed in the corresponding experiment.

Models	Atmospheric resolution (Lat × Lon)	Historical	Natural	GHG	RCP4.5	RCP8.5
ACCESS1-0	1.25° × 1.875°	√			√	√
ACCESS1-3	1.25° × 1.875°	√			√	√
BCC-CSM1-1	2.784° × 2.8125°	√	√	√	√	√
BCC-CSM1-1-m	1.112° × 1.125°	√			√	√
BNU-ESM	2.784° × 2.8125°	√	√	√	√	√
CanESM2	2.784° × 2.8125°	√			√	√
CCSM4	0.942° × 1.25°	√	√	√	√	√
CESM1-BGC	0.942° × 1.25°	√			√	√
CMCC-CM	0.75° × 0.75°	√			√	√
CNRM-CM5	1.397° × 1.406°	√	√	√	√	
CSIRO-Mk3-6-0	1.861° × 1.875°	√	√	√	√	√
FGOALS2-s	1.655° × 2.8125°	√			√	√
FIO-ESM	2.784° × 2.8125°	√			√	
GFDL-CM3	2.0225° × 2.5°	√	√	√	√	√
GFDL-ESM2G	2.0225° × 2.5°	√			√	√
GFDL-ESM2M	2.0225° × 2.5°	√	√	√	√	√
GISS-E2-H	2.0° × 2.5°	√	√	√	√	
GISS-E2-H-CC	2.0° × 2.5°	√			√	
GISS-E2-R	2.0° × 2.5°	√	√	√	√	√
GISS-E2-R-CC	2.0° × 2.5°	√			√	
HadGEM2-CC	1.25° × 1.875°	√			√	√
HadGEM2-ES	1.25° × 1.875°	√	√	√	√	√
INMCM4	1.5° × 2.0°	√			√	√
IPSL-CM5A-LR	1.895° × 3.75°	√	√	√	√	√
IPSL-CM5A-MR	1.268° × 2.5°	√			√	√
IPSL-CM5B-LR	1.895° × 3.75°	√			√	√
MIROC5	1.397° × 1.406°	√			√	√
MIROC-ESM	2.784° × 2.8125°	√	√	√	√	√
MIROC-ESM-CHEM	2.784° × 2.8125°	√	√	√	√	√
MPI-ESM-LR	1.861° × 1.875°	√			√	√
MPI-ESM-MR	1.861° × 1.875°	√			√	√
MRI-CGCM3	1.119° × 1.125°	√	√	√	√	√
NorESM1-M	1.895° × 2.5°	√	√	√	√	√

$$x_i = \sum_{j=i-n+1}^{j=i} \Delta_j \quad (2)$$

Third, the twelve time series x of each month (January to December) was fitted by the three-parameter log-logistic distribution that suggested by Vicente-Serrano et al. (2010). The probability density function $f(x)$ and cumulative distribution function $F(x)$ are listed below:

$$f(x) = \frac{\beta}{\alpha}\left(\frac{x-\gamma}{\alpha}\right)^{\beta-1}\left[1+\left(\frac{x-\gamma}{\alpha}\right)^{\beta}\right]^{-2} \quad (3)$$

$$F(x) = \left[1+\left(\frac{\alpha}{x-\gamma}\right)^{\beta}\right]^{-1} \quad (4)$$

where α, β, and γ are scale, shape and location parameters, respectively, which are estimated by the maximum likelihood method. Finally, the SPEI is calculated by transforming F to the standard normal distribution (φ) as Eq. (5).

$$SPEI = \varphi^{-1}(F) \quad (5)$$

According to its definition and calculation, the SPEI combines the sensitivity of the PDSI to changes in evaporative demand (Palmer, 1965) with the multiscalar nature of the SPI (McKee et al., 1993). Table 2 presents the categorization of dry and wet grades according to the SPEI as well as the corresponding cumulative probabilities relative to the base period (McKee et al., 1993; Yu et al., 2014).

Due to its multiscalar nature and ease of calculation, the SPEI has become popular and is widely used around the world in many aspects. For example, Vicente-Serrano et al. (2012) found the SPEI was superior to other drought indices for capturing the impacts of droughts on hydrologic, agricultural, and ecological variables from a global perspective. Huang et al. (2015) presented a method for predicting the mortality of trees in the Southwestern US based on the relationship between the SPEI and annual tree ring growth. Additionally, this index has also been used for drought assessment and monitoring works over many regions, such as in Southern Africa (Ujeneza and Abiodun, 2015), south Texas (Hernandez and Uddameri, 2014), Spain (López-Moreno et al., 2013), and China (Yu et al., 2014; Xu et al., 2015). SPEI was thus proposed for the analyses in this study. The SPEI, with a 12-month time scale, was calculated for each meteorological station from January 1951 to December 2014. The values for the months of December for all years were primarily used in this study (if not otherwise specified) because the 12-month SPEI in December well represents the cumulative precipitation deficits or wet/dry conditions for the entire year. The 12-month SPEIs were also calculated for CMIP5 models and their ensembles. The dry events with an SPEI < −1.0, including moderate drought, severe drought, and extreme drought, are discussed below.

To identify the role of anthropogenic activity on drought frequency change, the optimal fingerprint detection method is employed here that has frequently been used in recent years for detection and attribution analysis (e.g. Min et al., 2011; Zhang et al., 2013b; Sun et al., 2016). This method assumes that Y is expressed as the sum of scaled fingerprints X plus internal variability ε:

$$Y = \beta X + \varepsilon \quad (6)$$

where β are the scaling factors that estimated by the total least squares method (Allen and Stott, 2003; Min et al., 2011). If the computed scaling factor is positive and its associated 90% uncertainty range excludes zero, then detection is indicated (Min et al., 2011).

Furthermore, the detection analysis will be also performed on the drought frequency changes at different scales. The SPEI series are separated into two terms involving variability (inter-annual and inter-decadal variability) and long-term trend using the ensemble empirical mode decomposition (EEMD) method, which is an adaptive and temporally local filter developed in recent years (Wu and Huang, 2009). EEMD decomposed data $x(t)$ in terms of a set of components from high frequency to low frequency c_j, and the residual r_n:

$$x(t) = \sum_{j=1}^{n} c_j(t) + r_n(t) \quad (7)$$

The principle of the EEMD is simple, and the added white noise populates the whole time-frequency space uniformly with the constituting components of different scales (Wu and Huang, 2009). In this study, the variability term is obtained by summing the first five components from EEMD and summing the last two components as an adaptive nonlinear trend.

One should be pointed out here that some previous studies (e.g. Chen and Sun, 2015b) have indicated that the CMIP5 models generally performed poorly in simulating the variations of climate variables, particularly precipitation, but the observed long-term trends can be well captured by most models. To increase the robustness of the results in this study, three measures were taken to reduce the influence from these biases. First, the analyses in this study were carried out using the multi-model ensembles. Second, the detection and attribution analyses were implemented only among CMIP5 simulations, without reference to the observation. Third, the projections were primarily calculated from the differences among the periods of interest so that uncertainties sourced from internal models can be reduced.

Table 2
Categorization of dry and wet grades according to the SPEI and the corresponding cumulative probabilities relative to the base period.

Grades	SPEI	Cumulative probability
Extremely dry	Less than −2	0.0228
Severe dry	−1.99 to −1.5	0.0668
Moderate dry	−1.49 to −1.0	0.1587
Normal	−1.0 to 1.0	0.5000
Moderate wet	1.0 to 1.49	0.8413
Severe wet	1.5 to 1.99	0.9332
Extremely wet	Larger than 2	0.9772

3. Results

3.1. Hot drought events increased significantly in recent decades

Drought was analyzed in this study using the SPEI metrics; drought is considered to occur when the SPEI is less than −1.0. Fig. 2 presents the historical records of the SPEI, precipitation, and temperature variations for different regions in China for the period of 1951–2014. The values of precipitation and temperature here were calculated from the regional-weighted averages of all stations for each sub-region, and the SPEI series were calculated from the associated regional averaged precipitation and temperature. The drought events indicate a consistent increase for different regions in China over the past 60 years, coinciding with significant (at the 95% confidence level using the Mann-Kendall method) upward trends of temperature but no obvious changes in precipitation. Thus, an increasing number of hot droughts occurred under warm conditions. Additionally, the period of interest (1951–2014) was split into two periods, 1951–1994 and 1995–2014, to compare the dry conditions in China over the past two decades with earlier times.

Over NEC, the drought occurrences indicated by the SPEI showed an obvious increase over the past six decades, and the fre-

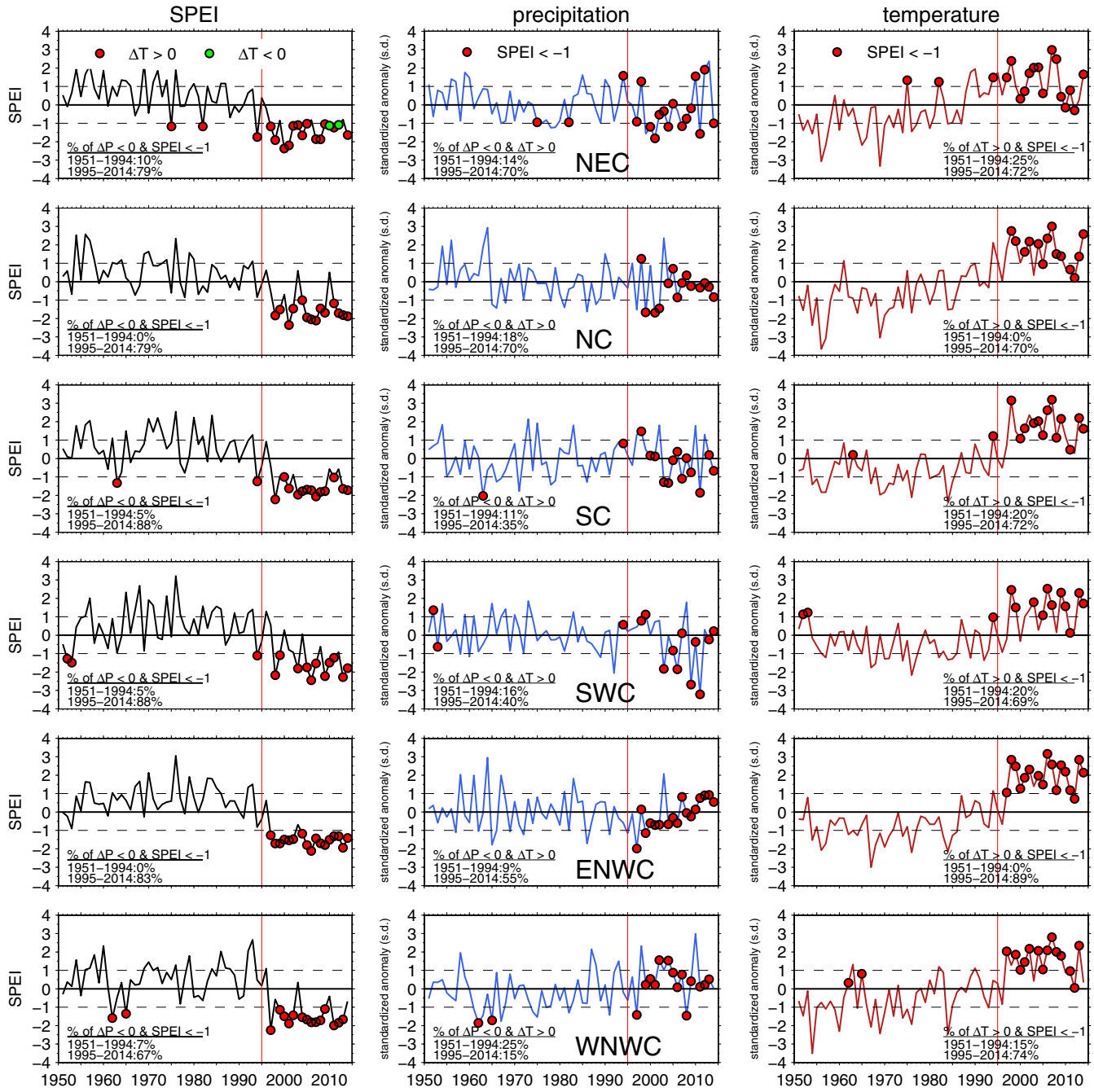

Fig. 2. Historical records of drought, precipitation, and temperature for different regions in China from 1951 to 2014. Droughts are represented by the December values of 12-month SPEI, and the standardized anomalies of precipitation and temperature are calculated as anomalies from the long-term annual mean, divided by the standard deviation of detrended historical annual anomaly time series. The circles in the panels indicate the years that suffered drought events with SPEI less than -1.0.

quency of years with SPEI < −1.0 was ten times greater in the most recent two decades (15 years in 1995–2014 = 75%) than in the preceding half century (3 years in 1951–1994 = 7%). This increase in drought occurrence was characterized by a substantial increase in low precipitation and high temperature (Figs. 2–4). According to the statistics, from 1951 to 1994 only 10% of the years had a negative precipitation anomaly that could produce an SPEI < −1.0 drought; however, this value increased to 79% in the most recent two decades (1995–2014). With a significant increase in air temperature, the probability of drought occurrence increased notably in the most recent two decades (72%) because of the high temperature anomaly, compared to earlier years (25%). Furthermore, the probability of a negative precipitation anomaly coinciding with a positive temperature anomaly has increased recently, with 14% of the years from 1951 to 1994 being classified as warm-dry compared with 70% of the years from 1995 to 2014. Most droughts have occurred under this warm-dry condition, especially recently, with 11 of 14 (79%) drought years during 1995–2014 occurring under this condition (Figs. 3 and 4).

In the regions of northern China, including NC and ENWC, droughts occurred mainly in 1995–2014, and no drought was observed in 1951–1994 on the basis of the SPEI indicator (Fig. 2).

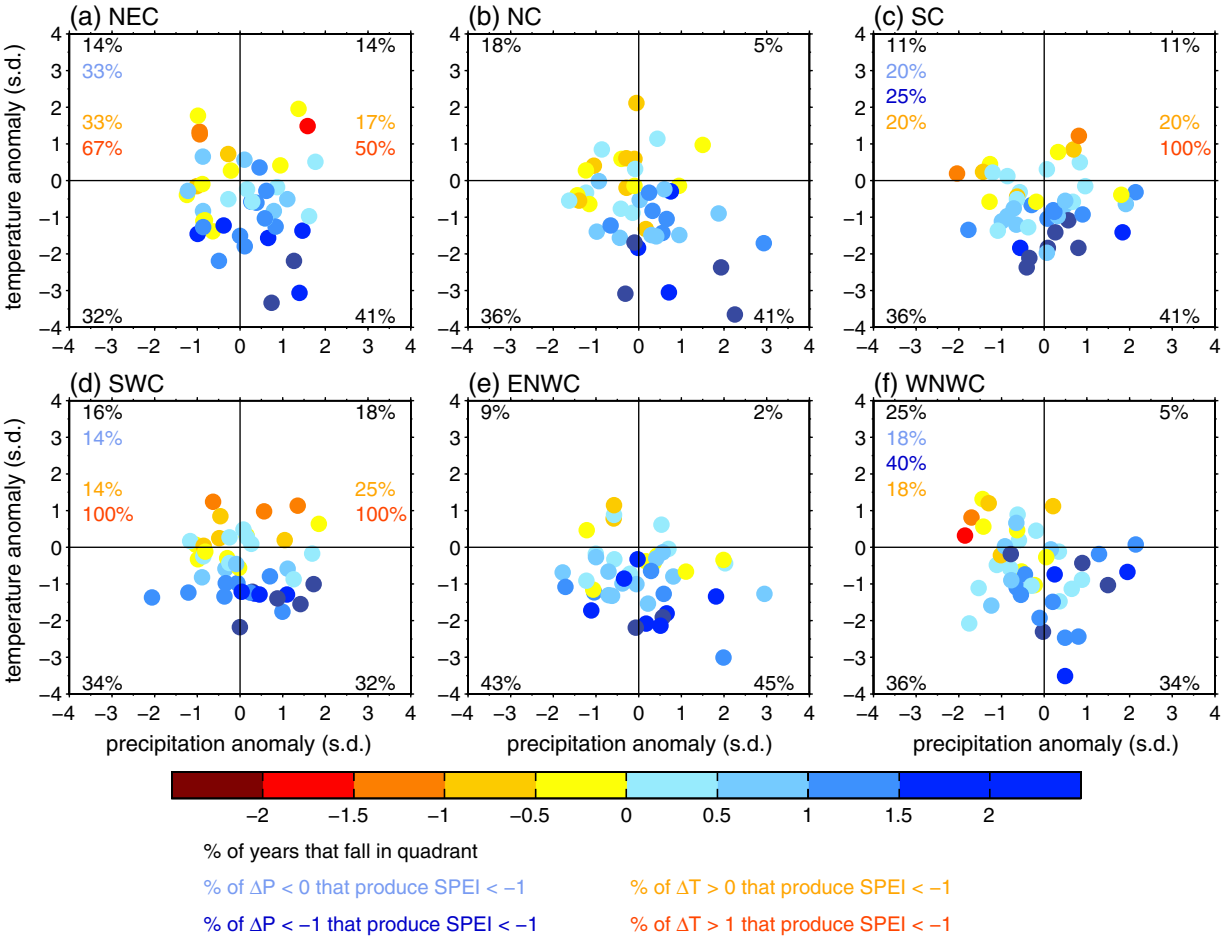

Fig. 3. Plots of relationships of drought occurrences with annual precipitation and temperature anomalies for the period 1951–1994 over (a) NEC, (b) NC, (c) SC, (d) SWC, (e) ENWC, and (f) WNWC. Warm colors mean negative SPEI values with high drought occurrence probability and cold colors represent positive SPEI values. Standardized anomalies are calculated as in Fig. 2. The percentage values shown in each quadrant are the percentage of years when droughts occurred under different precipitation and temperature criteria. The corresponding criteria are identified by different colors in the bottom of the figure.

There is almost no change in precipitation across these regions over the past 60 years, and even a slight increase was observed in the most recent two decades. The years with high temperature anomalies over NC increased from 23% in 1951–1994 to 100% in 1995–2014 and increased from 11% to 95% in ENWC, with no substantial corresponding changes in low precipitation anomalies, which were 54% of the years in 1951–1994 and 70% in 1995–2014 for NC and 52% in 1951–1994 and 60% in 1995–2014 for ENWC (Figs. 3 and 4). The probability of warm-dry conditions over these regions increased in the most recent two decades, 18% in NC and 9% in ENWC during 1951–1994 to 70% in NC and 55% in ENWC. Most droughts in the past two decades (79% in NC and 91% in ENWC) have taken place under these warm-dry conditions. This suggests that the increased probability of drought occurrence has resulted mainly from the significant warming of recent years.

The SPEI < −1.0 droughts over southern China, including SC and SWC, occurred relatively more frequently during 1995–2014, in 65% of these years in SC and 55% of these years in SWC (Fig. 2). Over southern China, the impact of a high temperature anomaly on drought obviously increased with this intensified warming, and positive temperature anomalies produced approximately 70% of the drought years in 1995–2014 compared with 20% of the years in 1951–1994. The probability of drought occurrence was also observed to increase due to the effect of a concurrent low precipitation anomaly. Only 5% of the years with a low precipitation anomaly could produce an SPEI < −1.0 drought in 1951–1994, but the probability increased to 88% in 1995–2014. With the increase in air temperature, the years under warm-dry conditions were also observed to increase, but the increased magnitudes were relatively smaller than in the northern regions of China. However, the SPEI < −1.0 droughts definitely occurred in these warm-dry years (Fig. 4).

Over the region of WNWC, a decadal shift from dry to wet conditions was reported to have occurred in the late 1980s (Chen et al., 2012b). With the increase in precipitation, there were just three years with negative precipitation anomalies during 1995–2014. However, of these three years, two years could produce an SPEI < −1.0 drought. The probability of a warm-dry year was observed to decrease when compared to the early period of 1951–1994, which differs from the other regions. Thus, the significant increase of SPEI < −1.0 drought (Fig. 2) mostly resulted from the increased air temperature in the most recent two decades (Fig. 2), and most of these droughts occurred under warm-wet conditions (Fig. 4).

Taken together, the historical records of the SPEI < −1.0 drought occurrences over different regions in China show a clear and consistent increase over the past 60 years, especially in the most recent two decades. Most of these increased droughts occurred under warm-dry conditions without a substantial corresponding change in precipitation, except for WNWC. Thus, the significant

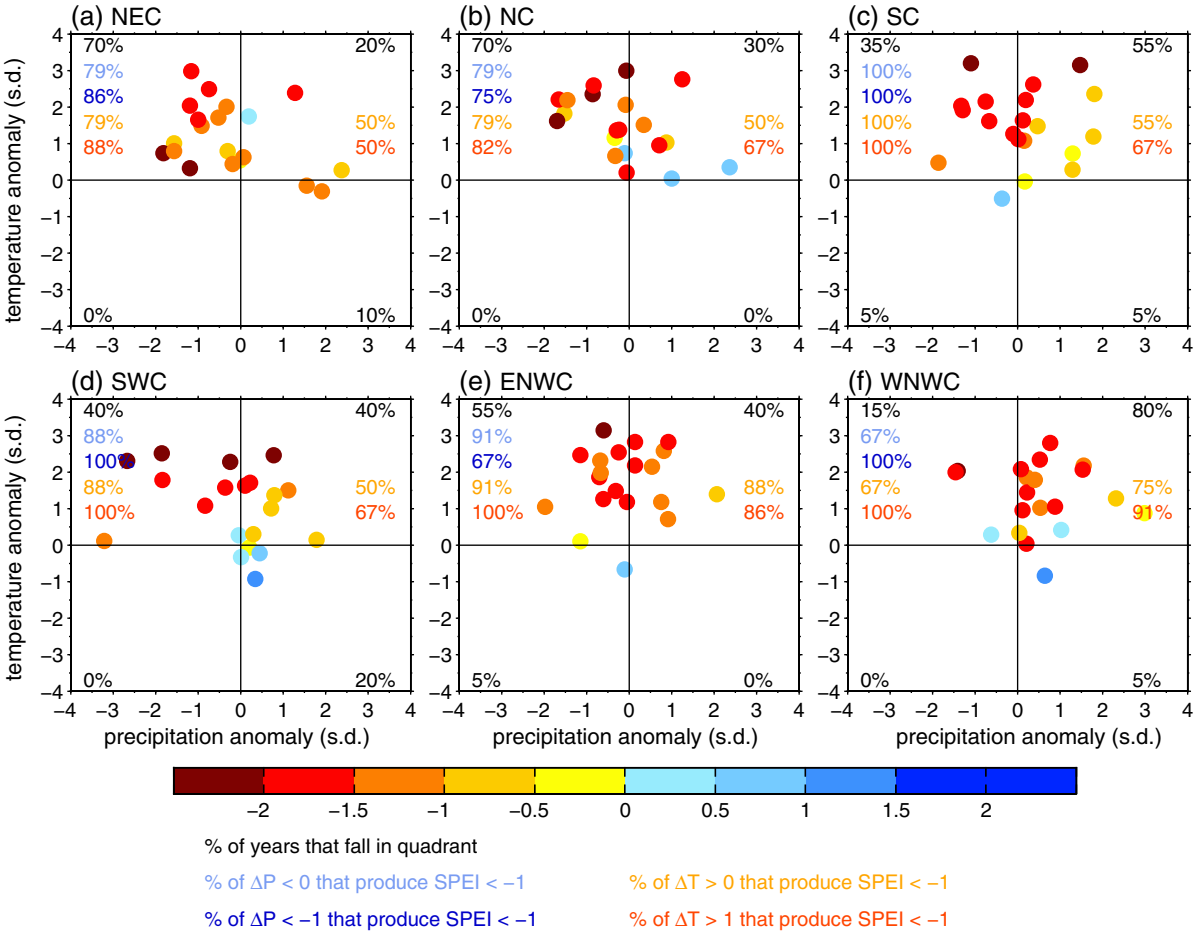

Fig. 4. Same as Fig. 3 but for the period 1995–2014.

warming across China is suggested as one of the main causes for the increased drought events although a precipitation deficit is still a prerequisite for drought occurrence.

3.2. Anthropogenic warming has increased hot drought events in the past decades

The recorded increasing trends of hot drought occurrences across China in the past decades are generally reproduced by the climate model simulations that include both natural and human forcings (Fig. 5), although the historical experiment exhibits a relatively weaker ability to simulate the inter-annual variations of SPEI. Thus, simulations from different CMIP5 experiments (including historical experiments, natural experiments, and GHG experiments) were analyzed to detect possible reasons for the increased hot drought occurrences across China in recent decades.

The fact that the air temperature across China has significantly increased in the last century (e.g., Ren et al., 2012; Cao et al., 2013) and that the warming clearly happens in the climate model simulations from both historical and GHG experiments but not in the simulations from the natural experiment (Figures not shown) suggest that human activity has caused substantial increases of air temperatures in China. Fig. 6 shows the temporal variations of SPEI for different regions in China from three CMIP5 experiments. As mentioned before, with rapid warming, the probability of hot droughts occurring has increased (decreasing trend for SPEI) across China, in accord with the climate model simulations that included the historical experiments. Similarly, this exacerbated trend of hot drought events was also observed in the simulations that included the GHG experiments for each region in China. The increasing trend was even relatively larger than that from the historical experiments, particularly in the most recent five decades. However, no trend was found in the simulations from the natural experiment. The same results can be obtained for the different regions across China, suggesting that human activity is one of the main causes for the obvious increase of hot drought occurrences in China in recent decades.

To further understand the possible reasons for the increasing probability of drought occurrences across China, Fig. 7 presents the temporal evolutions of the decomposed SPEI series by the EEMD method from three experiments over SC. Because similar evolutions and trends of the SPEI series could be found among the different regions across China (Fig. 6), we just took the decomposed results of SC as an example. The drying trend was clear in the simulations from the historical and GHG experiments, but not in the natural experiments. Furthermore, this drying trend was relatively larger in the GHG experiment than in the historical experiment result. However, the simulated strong inter-annual to inter-decadal variability of the SPEI series in the historical experiment could only be reproduced by the natural experiment, not by the GHG experiment. The estimated correlation coefficients of the variability components were up to 0.69 between the historical and natural experiments and −0.20 between the historical and GHG experiments. Additionally, similar magnitudes of variability for the SPEI series could be observed in the historical and natural results and were relatively larger than those in the GHG results. This suggests that the variability of droughts in this region was mainly affected by the natural variability while human activity

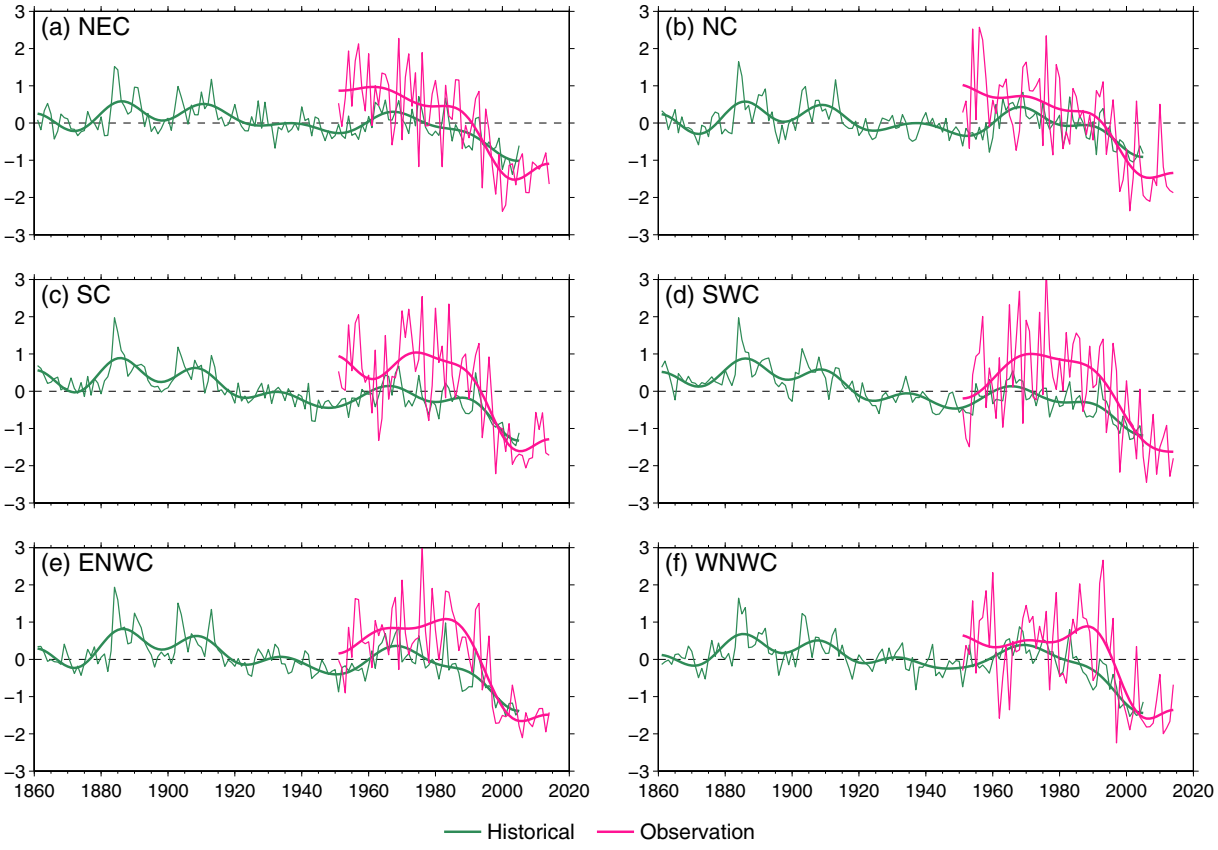

Fig. 5. Historical time series of the SPEI from the site observations (red line) and the ensemble-mean of 16 CMIP5 model simulations (green line) for different regions in China. Smoothed curves are the results after the 21-year low-pass filtering method was implemented.

played an important role in the drying trend over the last century in the region.

To confirm the aforementioned results, the optimal fingerprint detection method is used here. Fig. 8 shows the scaling factors and their 90% confidence intervals for different components of SPEI (presented in Fig. 7) over SC when the simulation from the historical experiment was regressed simultaneously onto a single signal (GHG or NAT) and two signals (GHG and NAT), respectively. Signals (GHG and NAT) were assessed to be detected by the 90% range of the scaling factors being above zero by both the single-signal and two-signal detection methods. However, the estimate of the NAT scaling factor was relatively larger than that for GHG (Fig. 8a). These estimations imply that the change of drought occurrence is mainly due to the combined activity of external natural forcings and anthropogenic activity, with a greater contribution from the effect of NAT than from GHG. In further analysis, the regional SPEI was separated into two series (i.e., inter-annual to inter-decadal variability and long-term trend), and the scaling factors for these two series were estimated using the two-signal and single-signal analysis, respectively (Fig. 8b and c). The best estimates of the GHG scaling factors were less than 0 both by the two-signal and single-signal methods for the impact on the variability, but the signals from the external natural forcings were indicated by the NAT scaling factors all being greater than 0.5 by these two methods (Fig. 8b). The results were the opposite when the detection analysis was applied to on the long-term trend (Fig. 8c). The best estimate of the GHG scaling factor was up to 0.49 and a relatively weaker signal was detected from the NAT, with a scaling factor at 0.22 using the two-signal analysis. However, no signal was detected from the NAT when the single-signal method was used (scaling factor less than 0), while the signal from the GHG was again robust with a scaling factor of 0.48. These estimations suggest that the impact of natural variability on drought is mainly from its effect on the inter-annual to inter-decadal variability of the external natural forcings and that human impacts were mainly responsible for the long-term drying trend over this region.

Natural variability and anthropogenic change are the two major drivers for drought occurrence changes over SC in the last century, but their impacts have varied depending on the time scale used. Natural variability was mainly responsible for the inter-annual to inter-decadal changes of drought events, and anthropogenic influences have been mainly responsible for the long-term drying trends, implying that anthropogenic warming has increased the hot drought risk and impact in this region. Similar results can be observed in the other regions across China (Figures not shown).

3.3. Hot drought events will become more frequent in the future

The influence of anthropogenic forcings on the droughts across China is significant. There is a high confidence level that the warming is projected to continue in the future, and the temperature in China may increase by 1.3–5 °C by the end of this century, which is a greater increase than that projected for the globe as a whole (Chen and Sun, 2015c). Given this background, how these droughts change has become a concern and key issue for the academic community, government, and the public.

Fig. 9 presents the probability distributions of future temperature, precipitation and drought occurrence changes over China under the RCP4.5 scenarios. The probabilities were calculated as the ratio of the number of models that meet the specified criteria to all models; thus, this also represents the confidence level of the projected result. From Fig. 9, it is clear that the probability of

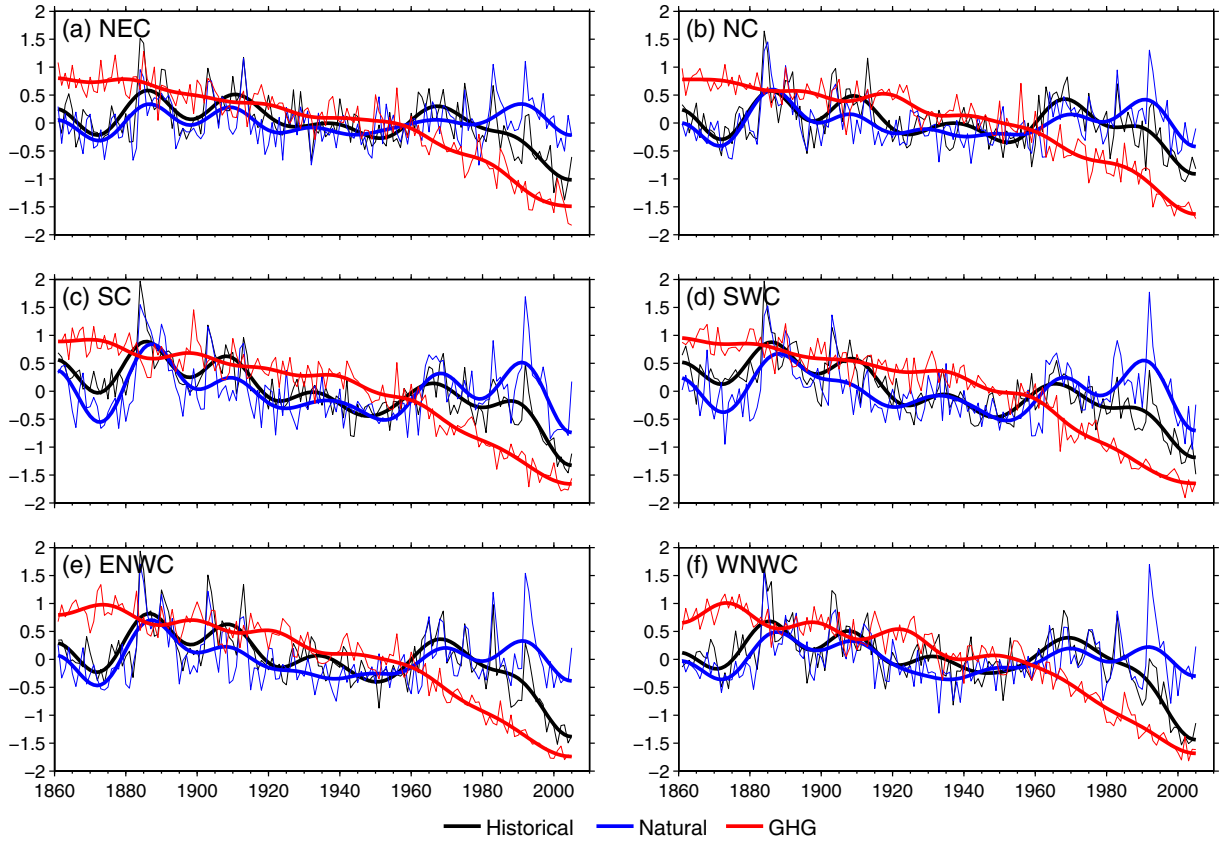

Fig. 6. Plots of the ensemble means of simulated SPEI for different experiments ("historical" experiment, "natural" experiment, and "GHG" experiment from CMIP5) for regions in China. The 21-year low-pass filtering results are represented by their corresponding smoothed curves.

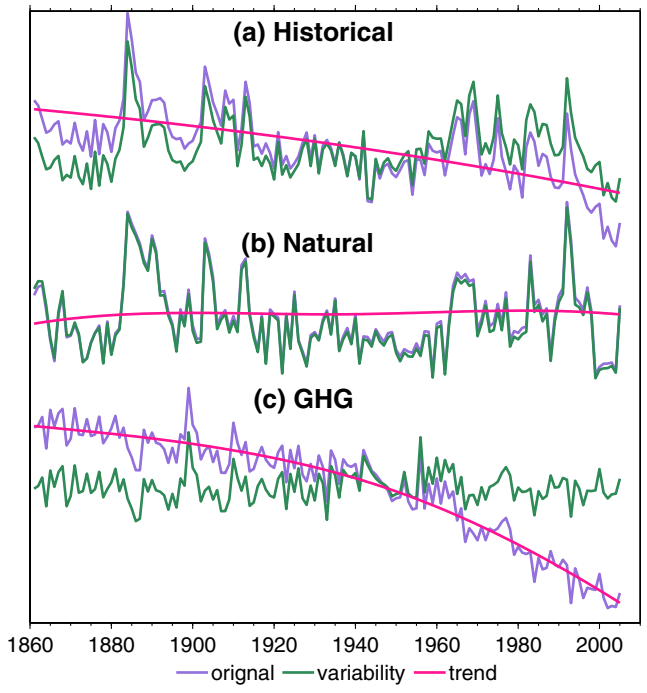

Fig. 7. Ensemble means of simulated SPEI over South China for the period 1861–2005 and their corresponding variabilities and trends (nonlinear) decomposed by the ensemble empirical mode decomposition (EEMD) method under (a) "historical", (b) "natural", and (c) "GHG" experiments.

extremely warm conditions (anomalies of 1 standard deviation) remains greatly elevated throughout this century, as indicated by early studies (e.g., Chen and Sun, 2015c). In China, the occurrence of warm years was observed to significantly increase, especially after ~1970, and reached 1.0 around the year 2010, which implies a transition to a permanently warm or extremely warm condition with a future risk of nearly 100%. However, the probability of a negative precipitation anomaly is projected to rapidly decrease beginning early in this century, suggesting an increase of annual precipitation in the future as indicated by earlier studies (e.g., Gao et al., 2012; Wang et al., 2012; Xu and Xu, 2012; Chen, 2013). Thus, the probability of simultaneous warm-dry conditions decreases with the probability of a negative precipitation anomaly. This shift from warm-dry to warm-wet conditions in the future still cannot mitigate the occurrence of droughts in China, despite the projected precipitation increase. The probability of drought years (SPEI < −1.0) has increased steeply since early in this century and will reach ~1.0 around the year 2050, suggesting that there would be nearly a 100% risk for drought occurrences, mainly due to high temperature anomalies in the future. This condition would be much worse according to the results of the RCP8.5 scenario (Fig. 10). The warming in China would progress much more rapidly in the RCP8.5 scenario than in RCP4.5, resulting in a higher probability of the occurrence of droughts in the future, and the probability of severe drought years (SPEI < −1.5) would be close to ~1.0 around the year 2080. The same analysis was implemented for six regions across China (Figures not shown) with similar results as above.

The projected changes of the occurrence probability of droughts (SPEI < −1.0) indicate increases across China, and all the grids would experience a nearly 100% risk of droughts by the end of this

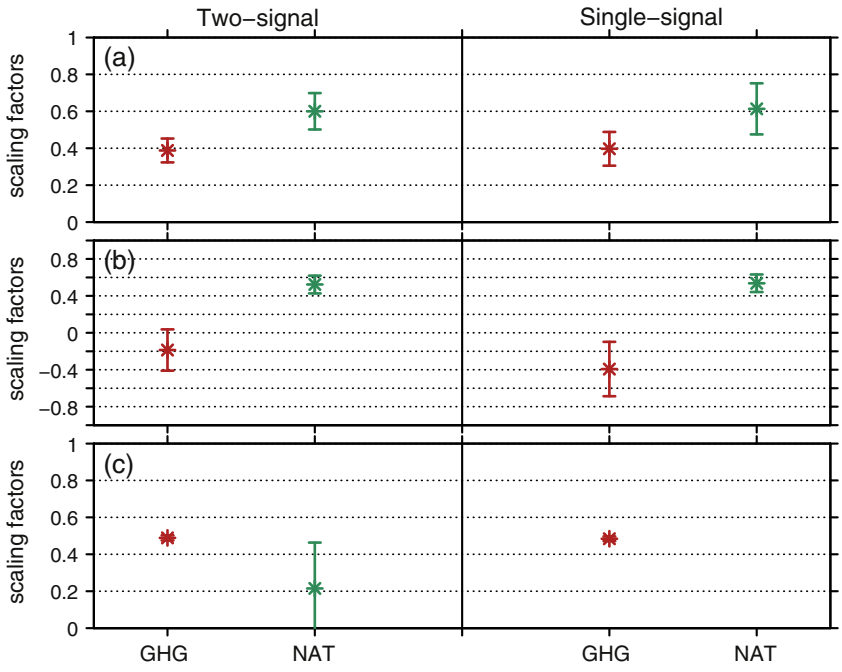

Fig. 8. Plots of scaling factors from single-signal (right) and two-signal (left) detection analyses for different components of SPEI over South China. (a) Original series of SPEI, (b) variability component, and (c) long-term trend component. The 5–95% confidence intervals of the scaling factors are displayed by the error bars.

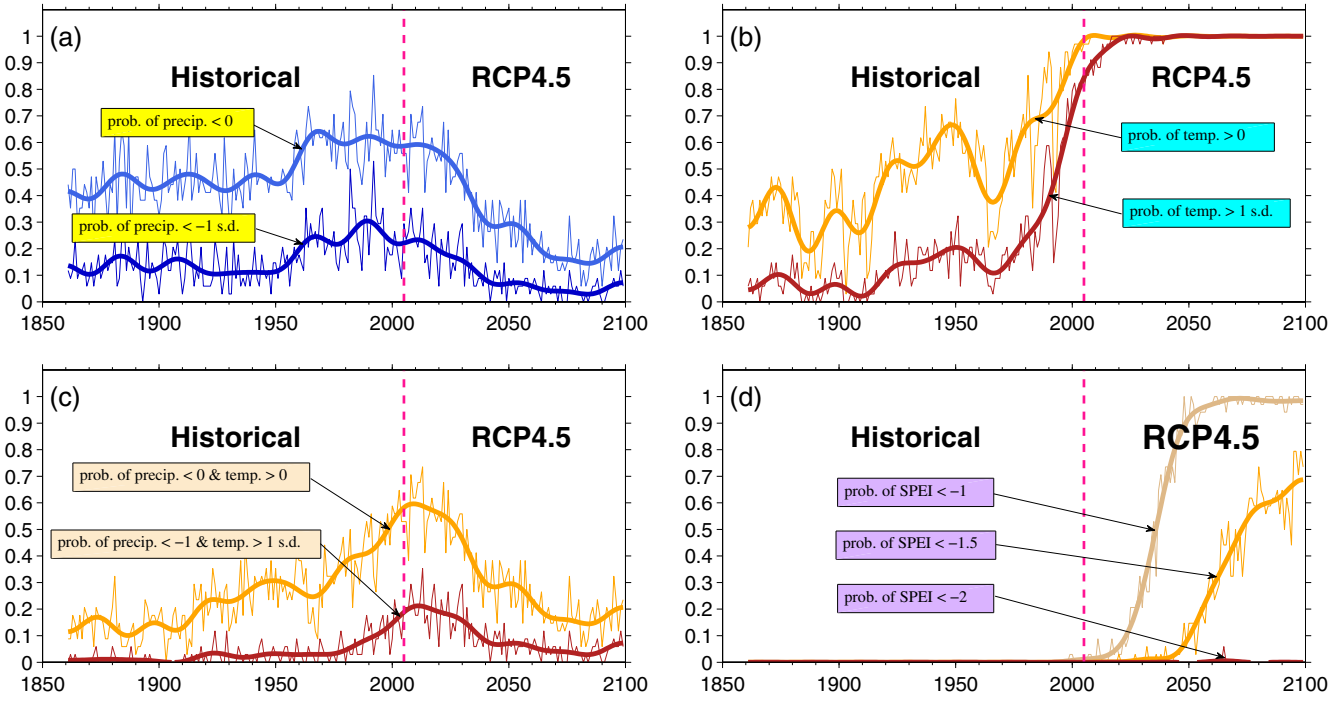

Fig. 9. Projected changes in the probability of hot drought occurrences in China in the 21st century from 33 CMIP5 models in the RCP4.5 scenario. (a) The probability of a negative annual precipitation anomaly that represents a dry condition, (b) the probability of a positive annual mean temperature anomaly that represents a warm condition, (c) the probability that a negative precipitation anomaly concurrent with a positive temperature anomaly, and (d) the probability of drought occurrences. The corresponding low-pass filtering results with a 21-year window are also shown in each panel. Probability is calculated as the percentage of models that meet the criteria listed in each panel, which also can reflect the uncertainty of the projected results from the CMIP5 models.

century (Figures not shown). Fig. 11 shows the ensemble changes of the occurrence probability of extreme droughts (SPEI < −2.0) across China at the end of this century relative to the period 1986–2005. Clearly, the probability of extreme drought occurrences is also increased all across China, especially in eastern China, with high reliability among models. Similar results can be found in the RCP8.5 scenario but with a relatively larger increase in the probability of occurrence.

Hot droughts will occur with a high probability in the future, even with precipitation increases across China. We consider this increasing trend of hot drought occurrence to be primarily attributable to continued anthropogenic warming in the future, and it will

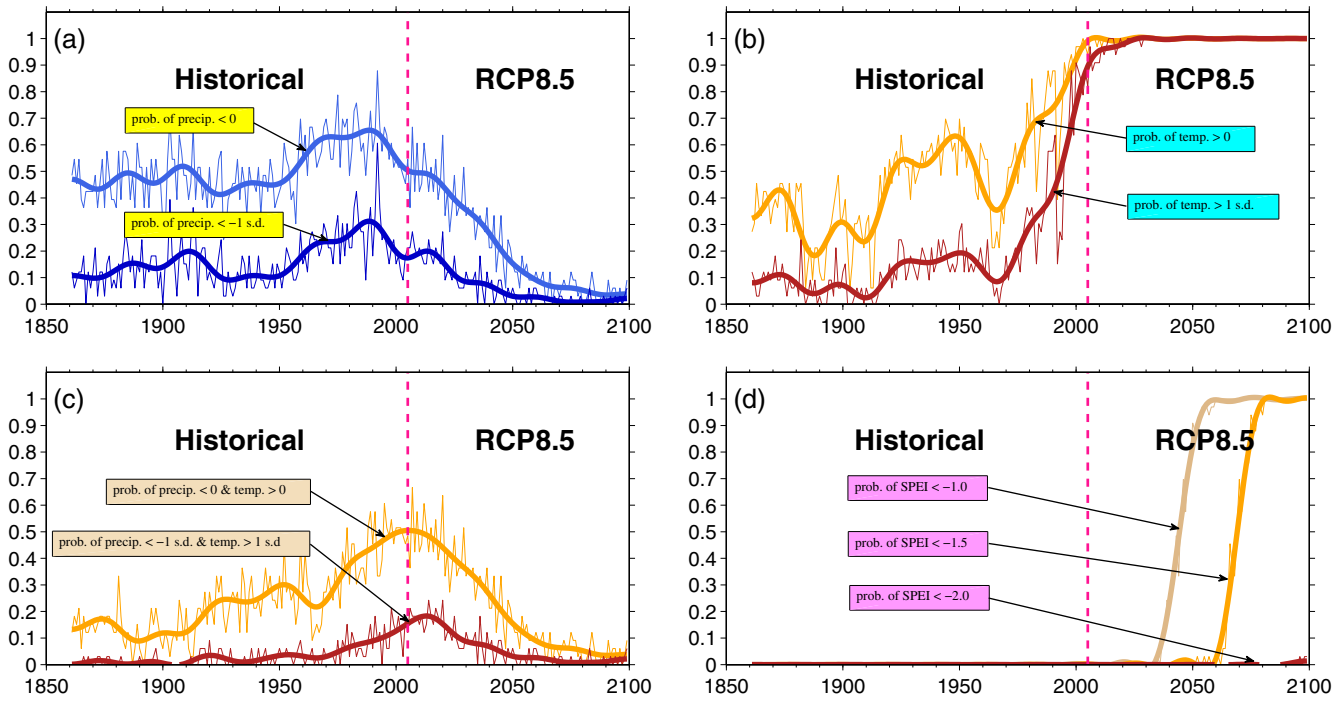

Fig. 10. Same as in Fig. 9 but from 28 CMIP5 models in the RCP8.5 scenario.

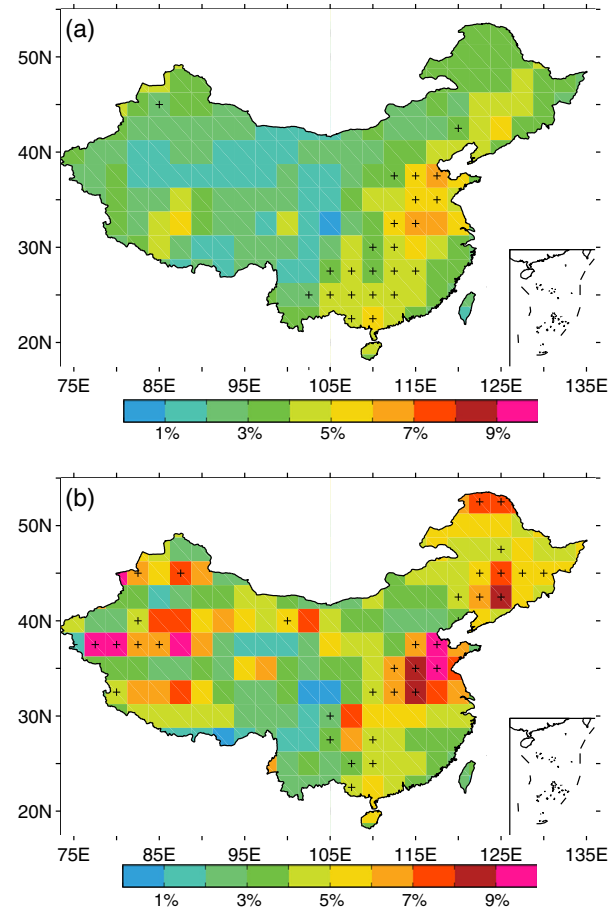

Fig. 11. Projected changes of extreme drought frequency (defined as the percentage of time in drought conditions, not percentage changes) from 1986–2005 to 2080–2099 under (a) RCP4.5 and (b) RCP8.5 scenarios. The extreme droughts are defined locally as monthly SPEI less than -2.0. The plus sign indicates at least 80% of the models agree on the sign of change.

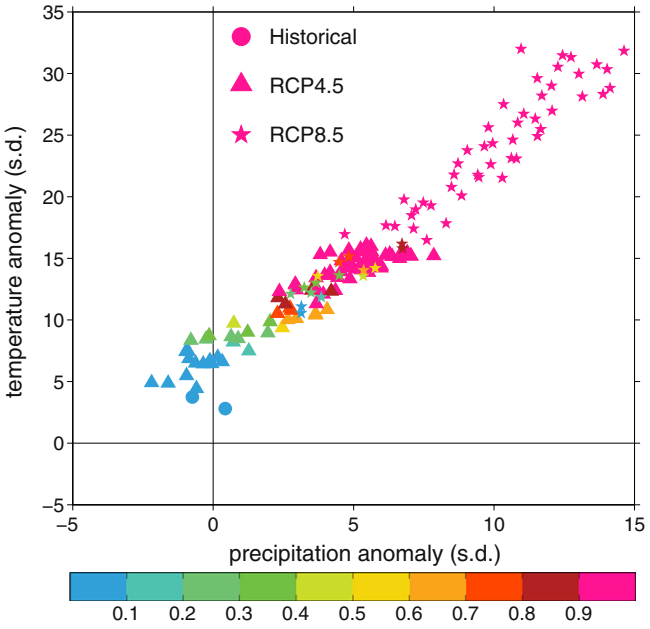

Fig. 12. Plots of the probability (calculated as in Fig. 9) of projected drought occurrences (SPEI < -1.0) in China in the 21st century and their relationships with precipitation and temperature anomalies.

always occur with high temperature anomalies. Thus, hot droughts would frequently happen under warm-wet conditions in the future (Fig. 12), unlike the warm-dry conditions in historical simulations and observations.

4. Discussion and conclusion

Given the severe impacts of droughts on human and natural systems, the drought occurrence changes across China were inves-

tigated using site observations for the last six decades. Our results suggest that the historical records of SPEI < −1.0 drought events present a consistent and obvious increase in occurrence across China in the past decades, especially in the most recent two decades. Most of these increased drought events occurred under warm-dry conditions with relatively high temperature anomalies but without large anomalies in precipitation. Thus, we can conclude that hot drought events have been observed to increase across China in the past decades. For example, over NEC, the probability of drought occurrence has substantially increased in the most recent two decades (72%) due to high temperature anomalies, which is a relatively larger increase than in previous decades (25% in the years 1951–1994). Furthermore, most droughts have occurred under warm-dry conditions, especially in 1995–2014, when 11 of 14 (79%) droughts occurred under this condition.

On the basis of CMIP5 simulations involving historical, natural, and GHG experiments, we suggest that the increase of hot drought occurrences across China results from the integrated activity of natural forcings and anthropogenic changes. However, their impacts vary for different time scales. Natural variability is mainly responsible for the inter-annual to inter-decadal changes in drought occurrences, and anthropogenic influences are mainly responsible for long-term drying trends, implying that anthropogenic warming has increased the hot drought events and has increased their risk and impact across China. With the projected continuous warming in the future, the probability of warm years is expected to increase significantly, with a transition to a permanently warm or extremely warm condition at a nearly 100% risk across China. Under this background, the SPEI < −1.0 droughts would occur with this near 100% risk by the year 2050, even though the future annual precipitation is projected to increase under the RCP4.5 scenario, and these conditions would become even worse under the RCP8.5 scenario. Thus, our results strongly suggest that anthropogenic warming has already increased the probability of hot drought occurrences and created major impacts on water policy, management, and infrastructure, and it will further increase hot drought risks and impacts across China in the future.

Some limitations of the current study should be acknowledged. For example, the evapotranspiration in SPEI is evaluated using the Thornthwaite algorithm (Thornthwaite, 1948). Some early studies (e.g., Sheffield et al., 2012) have indicated that the increase in global drought was overestimated when this simple equation was used, and the calculations would be more realistic if the more sophisticated Penman-Monteith method were used, which accounts for changes in available energy, humidity, and wind speed (Chen and Sun, 2015a). However, due to the limitations of the data availability, especially for the CMIP5 simulations involving natural and GHG experiments, we used the Thornthwaite equation instead of the Penman-Monteith method to calculate evapotranspiration in this study. Some previous works (e.g. Chen and Sun, 2015a) have indicated that the role of temperature is generally exaggerated for droughts when using the Thornthwaite equation in place of the Penman-Monteith method over the northern regions of China; however, almost no difference can be found for the southern regions of China. Thus, we believe that the results of this study will be robust, although the increase of droughts in response to anthropogenic warming may be somewhat overestimated for northern China.

Acknowledgements

We sincerely acknowledge the anonymous reviewers whose kind and valuable comments greatly improved the manuscript. This research was jointly supported by the National Key Research and Development Program of China (Grant No: 2016YFA0602401), the External Cooperation Program of BIC, Chinese Academy of Sciences (Grant No: 134111KYSB20150016), the National Natural Science Foundation of China (Grant No: 41305061), and the CAS—PKU Joint Research program.

References

AghaKouchak, A., Cheng, L., Mazdiyasni, O., Farahmand, A., 2014. Global warming and changes in risk of concurrent climate extremes: insights from the 2014 California drought. Geophys. Res. Lett. 41, 8847–8852. http://dx.doi.org/10.1002/2014GL062308.

Allen, M.R., Stott, P.A., 2003. Estimating signal amplitudes in optimal fingerprinting, Part I: Theory. Clim. Dyn. 21, 477–491.

Beguería, S., Vicente-Serrano, S.M., Reig, F., Latorre, B., 2014. Standardized precipitation evapotranspiration index (SPEI) revisited: parameter fitting, evapotranspiration models, tools, datasets and drought monitoring. Int. J. Climatol. 34, 3001–3023. http://dx.doi.org/10.1002/joc.3887.

Cao, L., Zhao, P., Yan, Z., Jones, P., Zhu, Y., Yu, Y., Tang, G., 2013. Instrumental temperature series in eastern and central China back to the nineteenth century. J. Geophys. Res. Atmos. 118, 8197–8207. http://dx.doi.org/10.1002/jgrd.50615.

Chen, H.P., Sun, J.Q., Wang, H.J., 2012a. A statistical downscaling model for forecasting summer rainfall in China from DEMETER hindcast datasets. Weather Forecast. 27, 608–628. http://dx.doi.org/10.1175/WAF-D-11-00079.1.

Chen, H.P., Sun, J.Q., Fan, K., 2012b. Possible mechanism for the interdecadal change of Xinjiang summer precipitation. Chin. J. Geophys. 55 (3), 267–274. http://dx.doi.org/10.1002/cjg2.1721.

Chen, H.P., 2013. Projected change in extreme rainfall events in China by the end of the 21st century using CMIP5 models. Chin. Sci. Bull. 58 (12), 1462–1472. http://dx.doi.org/10.1007/s11434-012-5612-2.

Chen, H.P., Sun, J.Q., Chen, X.L., 2013. Future changes of drought and flood events in China under a global warming scenario. Atmos. Oceanic Sci. Lett. 6, 8–13.

Chen, H.P., Sun, J.Q., 2015a. Changes in drought characteristics over China using the standardized precipitation evapotranspiration index. J. Clim. 28, 5430–5447. http://dx.doi.org/10.1175/JCLI-D-14-00707.1.

Chen, H.P., Sun, J.Q., 2015b. Assessing model performance of climate extremes in China: an intercomparison between CMIP5 and CMIP3. Clim. Change 129, 197–211. http://dx.doi.org/10.1007/s10584-014-1319-5.

Chen, H.P., Sun, J.Q., 2015c. Changes in climate extreme events in China associated with warming. Int. J. Climatol. 35, 2735–2751. http://dx.doi.org/10.1002/joc.4168.

Dai, A.G., Trenberth, K.E., Qian, T., 2004. A global dataset of Palmer drought severity index for 1870–2002: relationship with soil moisture and effects of surface warming. J. Hydrometeor. 5 (6), 1117–1130. http://dx.doi.org/10.1175/JHM-386.1.

Dai, A.G., 2012. Increasing drought under global warming in observations and models. Nat. Clim. Change 3 (1), 52–58. http://dx.doi.org/10.1038/nclimate1633.

Ding, Y., Sun, Y., Wang, Z., Zhu, Y., Song, Y., 2009. Inter-decadal variation of the summer precipitation in China and its association with decreasing Asian summer monsoon. Part II: possible causes. Int. J. Climatol. 29, 1926–1944. http://dx.doi.org/10.1002/joc.1759.

Dubrovsky, M., Svoboda, M.D., Trnka, M., Hayes, M.J., Wilhite, D.A., Zalud, Z., Hlavinka, P., 2009. Application of relative drought indices in assessing climate-change impacts on drought conditions in Czechia. Theor. Appl. Climatol. 96, 155–171. http://dx.doi.org/10.1007/s00704-008-0020-x.

Fu, C.B., Zeng, Z.M., 2005. Correlation between North Atlantic Oscillation index in winter and eastern China flood/drought index in the last 530 years. Chin. Sci. Bull. 50 (21), 2505–2516. http://dx.doi.org/10.1007/BF03183642.

Gao, H., Yang, S., 2009. A severe drought event in northern China in winter 2008–2009 and the possible influences of La Niña and Tibetan Plateau. J. Geophys. Res. 114, D24104. http://dx.doi.org/10.1029/2009JD012430.

Gao, X. J., D. Zhang, Z. Chen, J. S. Pal, and F. Giorgi, 2007: Land use effects on climate in China as simulated by a regional climate model. Sci. China (Series D: Earth Sci.), 50(4), 620–628, doi:10.1007/s11430-007-2060-y.

Gao, X.J., Shi, Y., Zhang, D., Giorgi, F., 2012. Climate change in China in the 21st century as simulated by a high resolution regional climate model. Chin. Sci. Bull. 57, 1188–1195. http://dx.doi.org/10.1007/s11434-011-4935-8.

Guttman, N.B., 1998. Comparing the Palmer drought severity index and the standardized precipitation index. J. Amer. Water Resour. Assoc. 34, 113–121. http://dx.doi.org/10.1111/j.1752-1688.1998.tb05964.x.

Hernandez, E.A., Uddameri, V., 2014. Standardized precipitation evaporation index (SPEI)-based drought assessment in semi-arid south Texas. Environ. Earth Sci. 71, 2491–2501. http://dx.doi.org/10.1007/s12665-013-2897-7.

Huang, K., Yi, C., Wu, D., Zhou, T., Zhao, X., Blanford, W.J., Wei, S.H., Wu, H., Ling, D., Li, Z., 2015. Tipping point of a conifer forest ecosystem under severe drought. Environ. Res. Lett. 10, 024011. http://dx.doi.org/10.1088/1748-9326/10/2/024011.

Li, C.X., Zhao, T.B., Ying, K.R., 2015a. Effects of anthropogenic aerosols on temperature changes in China during the twentieth century based on CMIP5 models. Theor. Appl. Climatol. http://dx.doi.org/10.1007/s00704-015-1527-6.

Li, X.Z., Zhou, W., Chen, Y.Q., 2015b. Assessment of regional drought trend and risk over China: A drought climate division perspective. J. Climate 28, 7025–7037.

López-Moreno, J.I., Vicente-Serrano, S.M., Zabalza, J., Beguería, S., Lorenzo-Lacruz, J., Azorin-Molina, C., Morán-Tejeda, E., 2013. Hydrological response to climate

variability at different time scales: A study in the Ebro basin. J. Hydrol. 477, 175–188.
Ma, Z.G., 2007. The interdecadal trend and shift of dry/wet over the central part of north China and their relationship to the Pacific decadal oscillation (PDO). Chin. Sci. Bull. 52 (15), 2130–2139. http://dx.doi.org/10.1007/s11434-007-0284-z.
Ma, Z.G., Fu, C.B., 2001. Trend of surface humid index in the arid area of northern China (in Chinese). Acta Meteor. Sin. 59, 737–746.
McKee, T. B., N. J. Doesken, and J. Kleist, 1993: The relationship of drought frequency and duration to time scales. Preprints, Eighth Conf. on Applied Climatology, Anaheim, CA, Amer. Meteor. Soc., 179–184.
Min, S.K., Zhang, X.B., Zwiers, F.W., Hegerl, G.C., 2011. Human contribution to more-intense precipitation extremes. Nature 470, 378–382. http://dx.doi.org/10.1038/nature09763.
Moss, R.H., Edmonds, J.A., Hibbard, K.A., Manning, M.R., Rose, S.K., van Vuuren, D.P., Carter, T.R., Emori, S., Kainuma, M., Kram, T., Meehl, G.A., Mitchell, J.F.B., Nakicenovic, N., Riahi, K., Smith, S.J., Stouffer, R.J., Thomson, A.M., Weyant, J.P., Wilbanks, T.J., 2010. The next generation of scenarios for climate change research and assessment. Nature 463, 747–756. http://dx.doi.org/10.1038/nature08823.
Palmer, W. C., 1965: Meteorological drought. U.S. Weather Bureau Research Paper 45, 58 pp.
Pei, L., Yan, Z.W., Yang, H., 2015. Multidecadal variability of dry/wet patterns in eastern China and their relationship with the Pacific Decadal Oscillation in the last 413 years (in Chinese). Chin. Sci. Bull. 60, 97–108.
Ren, G., Ding, Y., Zhao, Z., Zheng, J., Wu, T., Tang, G., Xu, Y., 2012. Recent progress in studies of climate change in China. Adv. Atmos. Sci. 29 (5), 958–977. http://dx.doi.org/10.1007/s00376-012-1200-2.
Sheffield, J., Wood, E.F., Roderick, M.L., 2012. Little change in global drought over the past 60 years. Nature 491, 435–440. http://dx.doi.org/10.1038/nature11575.
Song, F., Zhou, T.J., Qian, Y., 2014. Responses of East Asian summer monsoon to natural and anthropogenic forcings in the 17 latest CMIP5 models. Geophys. Res. Lett. 41, 596–603. http://dx.doi.org/10.1002/2013GL058705.
Sun, J.Q., 2014. Record-breaking SST over mid-North Atlantic and extreme high temperature over the Jianghuai-Jiangnan region of China in 2013. Chin. Sci. Bull. 59 (27), 3465–3470. http://dx.doi.org/10.1007/s11434-014-0425-0.
Sun, Y., Zhang, X.B., Ren, G.Y., Zwiers, F.W., Hu, T., 2016. Contribution of urbanization to warming in China. Nat. Climate Change. http://dx.doi.org/10.1038/NCLIMATE2956.
Thornthwaite, C.W., 1948. An approach toward a rational classification of climate. Geogr. Rev. 38, 55–94. http://dx.doi.org/10.2307/210739.
Ujeneza, E.L., Abiodun, B.J., 2015. Drought regimes in Southern Africa and how well GCMs simulate them. Clim. Dyn. 44, 1595–1609. http://dx.doi.org/10.1007/s00382-014-2325-z.
Vicente-Serrano, S.M., Beguería, S., López-Moreno, J.I., 2010. A multiscalar drought index sensitive to global warming: The standardized precipitation evapotranspiration index. J. Climate 23, 1696–1718. http://dx.doi.org/10.1175/2009JCLI2909.1.
Vicente-Serrano, S.M., Beguería, S., Lorenzo-Lacruz, J., Camarero, J.J., López-Moreno, J.I., Azorin-Molina, C., Revuelto, J., Morán-Tejeda, E., Sanchez-Lorenzo, A., 2012. Performance of drought indices for ecological, agricultural, and hydrological applications. Earth Interactions 16. http://dx.doi.org/10.1175/2012EI000434.1.
Wang, H.J., 2001. The weakening of the Asian monsoon circulation after the end of 1970s. Adv. Atmos. Sci. 18 (3), 376–386. http://dx.doi.org/10.1007/BF02919316.
Wang, H.J., 2002. The instability of the East Asian summer monsoon-ENSO relations. Adv. Atmos. Sci. 19 (1), 1–11. http://dx.doi.org/10.1007/s00376-002-0029-5.
Wang, H.J., Sun, J.Q., Chen, H.P., Zhu, Y.L., Zhang, Y., Jiang, D.B., Lang, X.M., Fan, K., Yu, E.T., Yang, S., 2012. Extreme climate in China: facts, simulation and projection. Meteorol. Z. 21, 279–304. http://dx.doi.org/10.1127/0941-2948-2012/0330.
Wang, H.J., He, S.P., 2015. The North China/Northeastern Asia severe summer drought in 2014. J. Climate. http://dx.doi.org/10.1175/JCLI-D-15-0202.1.
Wang, L., Chen, W., Zhou, W., Chan, J.C.L., Barriopedro, D., Huang, R.H., 2010. Effect of the climate shift around mid-1970s on the relationship between wintertime Ural blocking circulation and East Asian climate. Int. J. Climatol. 30, 153–158. http://dx.doi.org/10.1002/joc.1876.
Wang, L., Chen, W., Zhou, W., Huang, G., 2015. Understanding and detecting super extreme droughts in Southwest China through an integrated approach and index. Q. J. R. Meteorol. Soc. http://dx.doi.org/10.1002/pi.2593.
Wang, T., Wang, H.J., Otterå, O.H., Gao, Y.Q., Suo, L.L., Furevik, T., Yu, L., 2013. Anthropogenic agent implicated as a prime driver of shift in precipitation in eastern China in the late 1970s. Atmos. Chem. Phys. 13, 12433–12450. http://dx.doi.org/10.5194/acp-13-12433-2013.
Wu, Z., Huang, N.E., 2009. Ensemble empirical mode decomposition: A noise-assisted data analysis method. Adv. Adapt. Data. Anal. 1, 1–41. http://dx.doi.org/10.1142/S1793536909000047.
Xu, C.H., Xu, Y., 2012. The projection of temperature and precipitation over China under RCP scenarios using a CMIP5 multi-model ensemble. Atmos. Oceanic Sci. Lett. 5, 527–533.
Xu, K., Yang, D.W., Yang, H.B., Li, Z., Qin, Y., Shen, Y., 2015. Spatio-temporal variation of drought in China during 1961–2012: A climatic perspective. J. Hydrol. 526, 253–264.
Yang, J., Gong, D.Y., Wang, W.S., Hu, M., Mao, R., 2012. Extreme drought event of 2009/2010 over southwestern China. Meteorol. Atmos. Phys. 115, 173–184. http://dx.doi.org/10.1007/s00703-011-0172-6.
Yu, M., Li, Q., Hayes, M.J., Svoboda, M.D., Heim, R.R., 2014. Are droughts becoming more frequent or severe in China based on the Standardized Precipitation Evapotranspiration Index: 1951–2010? Int. J. Climatol. 34 (3), 545–558. http://dx.doi.org/10.1002/joc.3701.
Zhang, L.X., Zhou, T.J., 2015. Drought over East Asia: A review. J. Climate 28, 3375–3399. http://dx.doi.org/10.1175/JCLI-D-14-00259.1.
Zhang, W., Jin, F.F., Zhao, J.X., Qi, L., Ren, H.L., 2013a. The possible influence of a non-conventional El Niño on the severe autumn drought of 2009 in Southwest China. J. Climate 26, 8392–8405. http://dx.doi.org/10.1175/JCLI-D-12-00851.1.
Zhang, X.B., Wan, H., Zwiers, F.W., Hegerl, G.C., Min, S.K., 2013b. Attribution intensification of precipitation extremes to human influence. Geophys. Res. Lett. 40, 5252–5257. http://dx.doi.org/10.1002/grl.51010.
Zhao, T.B., Dai, A.G., 2015. The magnitude and causes of global drought changes in the twenty-first century under a low-moderate emissions scenario. J. Climate 28, 4490–4512.
Zhao, T.B., Li, C.X., Zuo, Z.Y., 2015. Contributions of anthropogenic and external natural forcings to climate changes over China based on CMIP5 model simulations. Sci. China: Earth Sci. http://dx.doi.org/10.1007/s11430-015-5207-2.
Zhou, T.J., Song, F., Lin, R., Chen, X., Chen, X., 2013. The 2012 North China floods: Explaining an extreme rainfall event in the context of a long-term drying tendency [in "Explaining extreme events of 2012 from a climate perspective"]. Bull. Amer. Meteor. Soc. 94 (9), S49–S51.
Zou, X.K., Gao, H., 2007. Analysis of severe drought and heat wave over the Sichuan Basin in the summer of 2006 (in Chinese). Adv. Clim. Chang. Res. 3, 149–153.